Journal of Fluorine Chemistry 132 (2011) 356–362

Contents lists available at ScienceDirect

Journal of Fluorine Chemistry

journal homepage: www.elsevier.com/locate/fluor

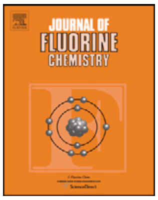

New hydrofluoropolyethers II: Physico-chemical characterization

Claudio Tonelli, Antonella Di Meo, Rosaldo Picozzi, Mattia Bassi [*]

Solvay Solexis S.p.A., V.le Lombardia 20, 20021 Bollate, Milano, Italy

A R T I C L E   I N F O

Article history:
Received 1 February 2011
Received in revised form 14 March 2011
Accepted 15 March 2011
Available online 23 March 2011

Keywords:
(1,1-Difluoroethoxy)fluoropolyethers
Hydrofluoropolyethers
Perfluoropolyethers
Physicochemical properties
Molecular weight
End-groups

A B S T R A C T

We obtained, through an original multi step synthetic approach with 60–80% selectivity, a novel family of hydrofluoropolyethers (HFPEs) characterized by a macromeric perfluoropolyether (PFPE) body end-capped, on one or both sides, by a 1,1-difluoroethoxy group. We synthesized these HFPEs trough an apparently conventional hydrogenation of PFPE precursors end-capped by reducible acyl halide groups and subsequent Cl cleavage by hydrogen, promoted by UV light in presence of hydrogen radical donor or by a metal catalytic system in presence of H_2. The physico-chemical properties of these HFPEs were described and compared to those of similar perfluorinated or partially hydrogenated molecules, obtaining master curves of general validity when temperature dependent properties, like viscosity, were compared under temperature reduced condition. The contribution of the end-groups to the specific property, vanishing at a sufficient high molecular weight, was demonstrated more and more important at the lowest oligomerization degrees.

1. Introduction

In recent years new partially fluorinated molecules have been synthesized and evaluated as possible alternative to the well established HFCs. Among them hydrofluoroethers (HFEs) became the subject of several studies [1–3]. They can be synthesized by different methods [4–19].

At present HFEs represent a possible alternative to HFCs because they are characterized by a good compromise between performances in use and environment protection. In fact, they combine a good set of properties with physico-chemical lability and reactivity. This latter characteristic guarantees a reduced lifetime in the troposphere so minimizing the undesired radical reactions in the stratosphere that represent the major drawback of CFC and HCFC molecules [20,21].

Among the new HFE candidates α,ω-(dihydro)fluoropolyethers (HFPEs) are a more recent and innovative class. They can be synthesised by a proprietary Solvay-Solexis technology, their physico-chemical properties can be tailored thanks to the easy modulation of their molecular weight by acting on the synthesis parameters or by appropriate distillation of the crude product. As a consequence, different grades of products, covering a wide range of boiling points, can be obtained and proposed to the market [22–25].

In a previous work this fruitful approach has been further on explored with the aim of finding new reaction routes, starting from functionalised fluoropolyethers, for the synthesis of new HFPEs [26].

Specifically, the synthesis of 1,1-(difluoroethoxy)fluoropolyethers and α,ω-bis[1,1-(difluoroethoxy)fluoropolyethers] has been described and a reaction pathway for their formation has been proposed, consistently with the observed selectivity and products analysis. The conversion of OCF_2COCl to OCF_2CH_3 previously described [26] is independent from the length and the structure of the chain bonded to the reactive centre, so that the proposed synthetic approach is of wide scope and applicability.

In the present work this synthesis has been extended by adding a further reaction step that allows the conversion of the alkyl chloride, if present, to the corresponding hydro derivative. New α-1,1(difluoroethoxy) ω-(hydro)fluoropolyethers have been so obtained, and their properties have been discussed and compared to understand the role of end groups in the physicochemical behaviour of this class of polyethers.

2. Results and discussion

2.1. Structures of the investigated products and of compounds used for comparison

Table 1 reports the structures of the synthesized HFPEs and their Cl-containing precursors.

The following compounds have been also discussed, for completeness of comparison:

R_f-$(OC_3F_6)_m(OCF_2)_n$-OR_f (where $R_f = -CF_3, -CF_2CF_3$) (Y-series) [27]

$CF_3(OC_2F_4)_p(OCF_2)_qOCF_3$ (Z-series) [27]

---

[*] Corresponding author. Tel.: +39 02 3835 6656; fax: +39 02 3835 6688.
E-mail address: mattia.bassi@solvay.com (M. Bassi).

0022-1139/$ – see front matter © 2011 Elsevier B.V. All rights reserved.
doi:10.1016/j.jfluchem.2011.03.013

Table 1
Structures and molecular weights of HFPE series: (1,1-difluoroethoxy)fluoropolyethers (from H-n_1 to H-n_5), α-(difluoroethoxy) ω-(hydro)fluoropolyethers (from 2H-n_2 to 2H-n_5), and α,ω-bis[1,1-(difluoroethoxy)fluoropolyethers] (H-Z).

Product[a]	Product
H-n1	$ClCF_2CF(CF_3)OCF_2CH_3$
H-n2	$Cl(C_3F_6O)_2CF_2CH_3$[a]
H-n3	$Cl(C_3F_6O)_3CF_2CH_3$[a]
H-n4	$Cl(C_3F_6O)_4CF_2CH_3$[a]
H-n5	$Cl(C_3F_6O)_4CF(CF_3)OCF_2CH_3$[a]
2H-n2	$H(C_3F_6O)_2CF_2CH_3$[b]
2H-n3	$H(C_3F_6O)_3CF_2CH_3$[b]
2H-n4	$H(C_3F_6O)_4CF_2CH_3$[b]
2H-n5	$H(C_3F_6O)_4CF(CF_3)OCF_2CH_3$[b]
H-Z	$CH_3CF_2O(CF_2CF_2O)_2CF_2CH_3$

[a] $ClCF_2CF(CF_3)$– = 30%; $CF_3CF(Cl)CF_2$– = 70% (molar base).
[b] $HCF_2CF(CF_3)$– = 30%; $CF_3CF(H)CF_2$– = 70% (molar base).

$HCF_2(OC_2F_4)_p(OCF_2)_qOCF_2H$ (HFPE-series)[3]
$CH_3(OC_2F_4)_p(OCF_2)_qOCH_3$ (CH_3OZ-series) [28]

Chemical structures of products and comparative compounds are identified by letters and digital numbers. Letters are diagnostic for the identification of the chemical class, whereas digital numbers parallel the increasing molecular weight.

Y- and Z-series are representative of perfluoropolyethers commercially known with trade names Fomblin® and Galden® from Solvay Solexis, and have been included to compare the effect of perfluorinated chain ends to the partially or completely hydrogenated end groups. The differences with the properties of other industrial perfluoropolyethers with similar structures (e.g., Krytox® from Du Pont [29] and Demnum® from Daikin [30]), have already been extensively discussed [27].

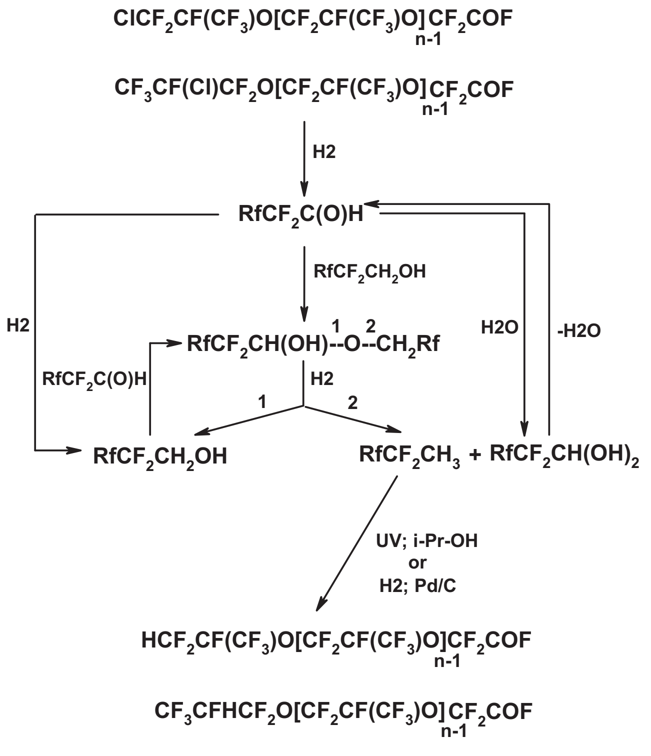

Scheme 1.

Table 2
Glass transition temperature, specific volume, viscosity and dielectric constant as a function of structure and molecular weight for HFPE series compared with other series.

Compound	Mn[a]	H[b] (ppm)	T_g (K)	Specific volume (cc/g)	η 20 °C (mPa s)	ε (1 kHz)
HFPE-1	228	8800	117	0.641	0.58	5.2
HFPE-2	342	5900	126	0,617	0.96	4.4
HFPE-3	479	4200	131	0.595	1.50	3.6
HFPE-4	655	3100	136	0.581	2.58	3.1
CH_3O-Z_1	162	37,000	–[c]	0.766	0.73	n.a.
CH_3O-Z_2	278	21,600	146[d]	0.680	1.27	5.9
CH_3O-Z_3	394	15,200	151[e]	0.653	1.46	6.6
CH_3O-Z_4	460	13,000	145	0.633	1.69	6.2
H-n_1	267	11,200	121[f]	0.669	0.76	5.9
H-n_2	432	6900	140	0.607	1.75	4.0
H-n_3	599	5000	153	0.587	3.36	4.0
H-n_4	765	3920	164	0.566	6.56	3.1
H-n_5	931	3200	163–171	0.541	10.2	3.0
2H-n_2	398	10,000	145	0.630	1.79	4.1
2H-n_3	564	7100	157	0.596	3.26	3.6
2H-n_4	730	5500	166	0.576	6.21	3.2
2H-n_5	896	4500	174	0.574	9.13	3.2
H-Z	378	15,900	145[g]	0.870	2.2	7.9
Y1	753	0	142	0.561	3.5	–
Y2	1109	0	174	0.539	31.3	–
Y3	1199	0	182	0.536	48.7	–
Y4	1801	0	188	0.532	115.7	–
Y5	2467	0	196	0.529	249.6	–
Y6	3260	0	195	0.527	498.6	–
Y7	6530	0	208	0.523	2806	–
Z1	1800	0	134	0.581	2.54	–
Z2	3581	0	137	0.547	53.4	–
Z3	7087	0	140	0.544	280.2	–
Z4	9684	0	142	0.542	432	–
Z5	11,892	0	141	0.541	1096	–

[a] Molecular weight (Mn) determined by ^{19}F NMR.
[b] Hydrogen content calculated from the molecular structure.
[c] A melting point at 252 K (10.7 kJ/mol) is observed.
[d] An additional melting point at 209 K (0.3 kJ/mol) is observed.
[e] An additional melting point at 239 K (22.0 kJ/mol) is observed.
[f] An additional melting point at 184 K (6.8 kJ/mol) is observed.
[g] An additional melting point at 195 K (0.5 kJ/mol) is observed.

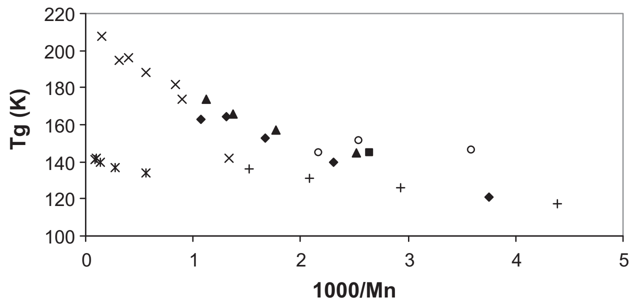

Fig. 1. Dependence of T_g on molecular weight: ◆ H-n-series; ▲ 2H-n-series; ■ H-Z; × Y-series; * Z-series; + HFPE-series; ○ CH_3OZ-series.

2.2. 2H-n-series synthesis route

Among the different structures investigated in the present work, 2H-n-series is new and obtained by an original multi step process. The first step of the reaction scheme, already described in a previous work, is common with H-Z and H-n-series, and it consists of an apparently conventional catalytic hydrogenation of PFPE precursors end-capped by reducible acyl chloride groups. However, the analysis of both yield and by-products structures, together with experiments devoted to the elucidation of the reactivity of possible intermediates, confirm that an unconventional reaction pathway is effective. In fact, the target product is obtained by hydrogenolysis of the addition product between two key intermediates: aldehyde and alcohol [26].

The second step makes possible to substitute chlorine atoms, if present in the precursor, by hydrogen. This goal can be achieved according to two different procedures, whose choice depends on the boiling point (i.e., volatility) of the PFPE intermediate. When low boiling intermediates are considered a photo activated Cl abstraction is performed at room temperature in presence of a hydrogen donor; while, for high boiling intermediates a catalytic hydrogenolysis at high temperature is conveniently performed.

The following Scheme 1 summarizes the overall reaction multi step process for the synthesis of 2H-n-series.

2.3. Physicochemical characterization

Table 2 shows some physicochemical properties of H-n_{1-5}, $2H_{n2-n5}$ series and H-Z, compared to the values previously measured on the other series [3,27,28].

The correlation between T_g and molecular weight (fig. 1) is well represented by Eq. (1), as firstly proposed by Fox and Flory [31]:

$$T_g = T_{g\propto} - \frac{A}{\text{Mn}} \qquad (1)$$

in which T_g and $T_{g\propto}$ are the glass transition of a polymer of average numerical molecular weight equal to Mn and infinite, respectively; while A is a specific constant for the investigated polymeric structure.

H-n and 2H-n series confirm the trend already observed for analogous PFPE-based oligomers: a single value of $T_{g\propto}$ can be attributed to the common perfluorinated body. Specifically, a negative slop is observed in both cases, similarly to the behaviour observed for unfunctionalized oligomers (Y-series). The calorimetric properties of these molecules, and their dependence on the temperature, are thus dominated by the internal fluorinated body, whereas the contribution of the end-units to the overall cohesive interaction is negligible. Y, H-n- and 2H-n-series lay on the same master curve, confirming the prevalent effect of internal PFPE structure over the terminal groups when these are unable to form strong non covalent interactions, e.g., hydrogen bonding among hydroxyl groups.

The limiting glass transition values increases from ca. 145–150 K to 216 K when all (OCF_2CF_2) and (OCF_2) (C_1 and C_2 units, respectively), typical of linear PFPE series (Z, HFPE), are substituted with –(OCF_2CFCF_3) repeating units (Y and H-n or 2H-n series). This effect is generally attributed to the “stiffening” of the chain segments whose cooperative motions originate the glass transition phenomenon [32].

Also the behaviour of HFPE-series confirms that the contribution of the internal PFPE body is dominant respect to the ability of H-containing terminal groups to promote hydrogen bonding formation.

The unexpected trend of CH_3OZ-series can be, at least partially, attributed to some structural heterogeneity within this series. In fact, only sample CH_3O-Z_4 contains a (OCF_2) unit (i.e., $q = 1$ in the formula). This very flexible segment contributes to a significant reduction of the T_g of the molecule [33,34]. Moreover, apart from CH_3O-Z_4, which forms a completely amorphous solid phase, the other terms of this series are well ordered oligo(OCF_2CF_2) chains with a strong tendency to crystallize (see notes c–e to Table 2), thereby promoting a sensible increase in the glass transition of the amorphous phase, as it is evident by comparison with analogous H-n and 2H-n series.

As a consequence of the above consideration, it is clear that, for all series compared in the present work, the structure stiffness is ruled by the internal backbone, with special reference to the C/O ratio, and presence of pendant CF_3 groups, while the slight polarity increase exerted by the insertion of single H atom, methyl or methoxy groups plays a secondary, or even negligible role. Therefore, two master curves, related to linear and branched molecules, well describe the whole series here considered.

The specific volume (Fig. 2) of all series at high molecular weights converge towards two, very close, asymptotic values: 0.54 ml/g and 0.52 ml/g for linear PFPE chain (Z-series) and branched PFPE chain (Y-series), respectively. In the low molecular weight region, the limiting values are strongly dependent on the end-groups nature, with special emphasis on its hydrogen content. For instance, the contribution of CH_3 end-groups to the specific volume increase is much higher than the similar contribution of perfluoroalkylic end-group (see for comparison H_n-series and Y-series; and also CH_3O-series and Z-series). When very low Mn are considered the contribution from the free volume introduced by the end-groups overcomes the contribution of the PFPE chain structure. H-n-series and 2H-n-series show higher specific volume than HFPE-series, in spite of the fact that branched PFPE chain should have lower specific volume than linear PFPE chain, as it is indicated by the different asymptotic value above discussed.

The isothermal viscosity data reported in the semi-logarithmic graph of Fig. 3 shows some very interesting features. The expected monotonic trend for the relationship between viscosity and molecular weight is generally confirmed. All hydrogen containing

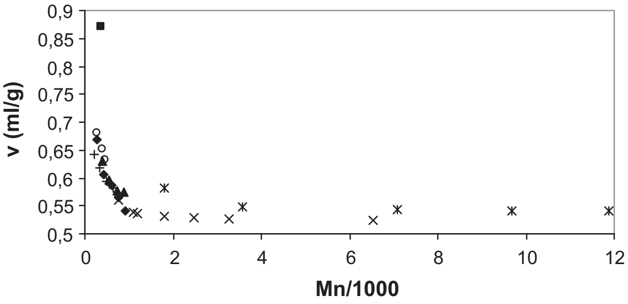

Fig. 2. Dependence of the specific volume (v) on molecular weight: ◆ H-n-series; ▲ 2H-n-series; ■ H-Z; × Y-series; * Z-series; + HFPE-series; ○ CH_3OZ-series.

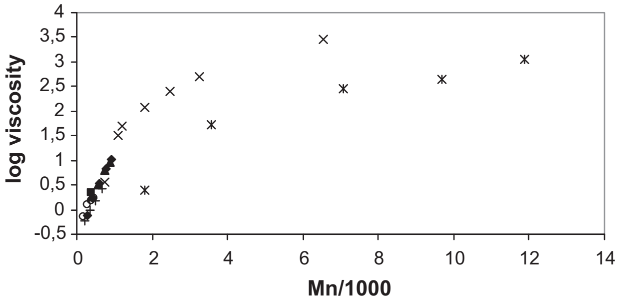

Fig. 3. Dependence of the viscosity on molecular weight: ◆ H-n-series; ▲ 2H-n-series; ■ H-Z; × Y-series; * Z-series; + HFPE-series; ○ CH_3OZ-series.

molecules, independently from the structure of the internal PFPE body, belong to the same master curve. This evidence confirms that, when low molecular weights are considered, the contribution of end groups becomes important. The higher polarity of these partially fluorinated molecules, compared to the perfluorinated ones, increases the intermolecular associations among dipoles; that, in turn, gives higher viscosity values. This feature is well evident when the viscosity of partially fluorinated molecules is compared to that of linear perfluorinated molecules (Z-series). Smaller differences are observed for a similar comparison with the higher viscous Y-series, that roughly belongs to the same semi-logarithmic master curve; even if, also in this case, when similar molecular weights are compared, H-containing molecules show higher viscosity, independently from the nature (linear or branched) of their fluorinated internal body.

It should be expected that, above a critical molecular weight, the contribution of end-groups tends to vanish and the viscosity will be ruled by the structure of the PFPE body.

As a consequence, above this critical value, two master curves are expected to describe the behaviour of all series, independently from the presence of different chain-ends. One curve, at higher viscosity, corresponds to branched structures, while the other, at lower viscosity, relates to the linear families.

In Fig. 4 viscosity data of H-n_1, $HFPE_{HG\text{-}20}$ and CH_3O-Z_2 vs. temperature are represented. These three molecules have been selected and compared because of their similar molecular weight but different hydrogenated end-groups. As the investigated temperature range lies at the extreme limit for the application of the Williams, Landel and Ferry's equation [36], the relationship between viscosity and temperature has been described by the well-known Arrhenius equation (2):

$$\eta = A \exp \frac{\Delta E_\eta}{RT} \qquad (2)$$

Activation energy for the viscous flow (ΔE_η) has been calculated for all samples, and values of 12.0 kJ/mol, 9.1 kJ/mol and 15.8 kJ/mol, have been obtained for H-n_1, $HFPE_{HG\text{-}20}$, and CH_3O-Z_2, respectively. All viscosity data seem to merge together when the temperature reaches a value of ca. 350 K, whereas significant differences among these structures are observed at lower temperatures. These differences could be preliminarily attributed to the structural diversification (i.e., differences in end-groups and internal fluorinated chain), which could rule the viscosity dependence on the temperature. However, these results could also relate to the change of free volume with temperature, because the so-called "frictional coefficient" also changes with temperature [36]. A state of iso-free volume can be obtained simply by comparing viscosities of samples that are not at the same temperature, but at the same value of ($T - T_g$); these data are represented in Fig. 5. This approach allows the evaluation of the contribution of different end-groups to the viscosity in the explored temperature range. In this case H-n1 and CH_3O-Z_2, both characterized by a CH_3 end-group, merge together in all the explored temperature range, and a single master curve well describes their viscosity behaviour as a function of temperature. While, $HFPE_{HG\text{-}20}$, terminated by a CF_2H group, performs slight differently; this different end-group structure could justify the observed trend. However, it cannot be excluded that the presence of small crystalline phases in all samples, characterized by different melting temperature, but always well below the lowest selected experimental temperature (230 K) may play a certain role, by changing the cohesive energy density of the compounds.

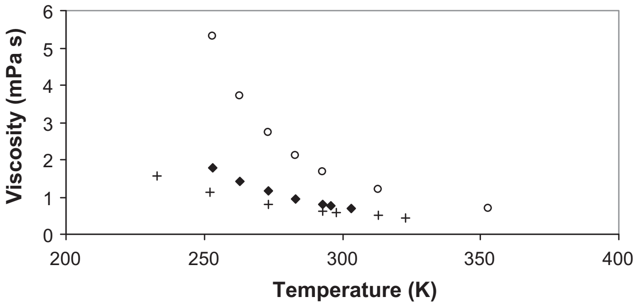

Fig. 4. Viscosity as a function of the temperature: ◆ H-n1; + $HFPE_{HG\text{-}20}$*; ○ CH_3O-Z_2; *This molecule has a HFPE structure but average MW 250 [35].

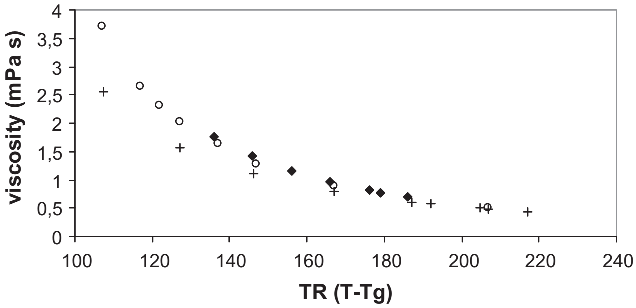

Fig. 5. Viscosity as a function of the reduced temperature: ◆ H-n1; + $HFPE_{HG\text{-}20}$*; ○ CH_3O-Z_2. *This molecule has a HFPE structure but average MW 250 [35].

The viscosity data of 2H-n-series, represented vs. temperature in Fig. 6, seem to merge at temperatures above 300 K, whereas very significant differences among these structures are observed at lower temperatures. These differences could be attributed both to the molecular weight change within the series and to the change of free volume with temperature [37]. The activation energy for the viscous flow (ΔE_η) has been calculated also for this series; values of 16.3 kJ/mol, 22.0 kJ/mol, 24.3 kJ/mol and 28,5 kJ/mol, moving from the lower to the higher molecular weight, have been obtained.

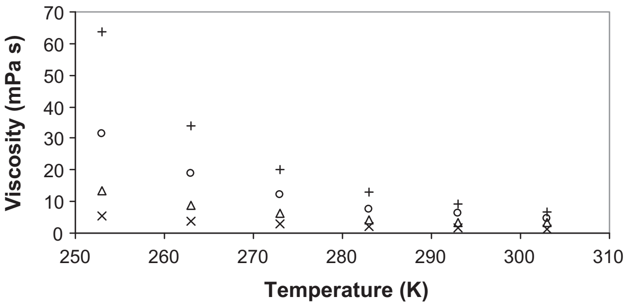

Fig. 6. Viscosity as a function of the temperature: × 2H-n_2; △ 2H-n_3; ○ 2H-n_4; + 2H-n_5.

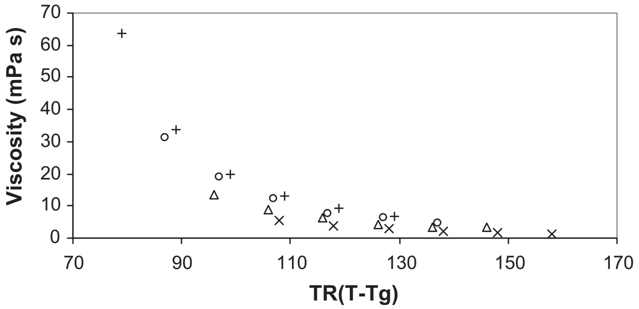

Fig. 7. Viscosity as a function of the reduced temperature: × 2H-n_2; △ 2H-n_3; ○ 2H-n_4;+ 2H-n_5.

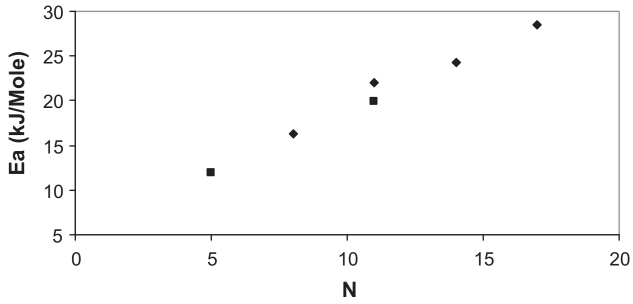

Fig. 8. Activation energy of viscous flow (E_a) as a function of the number of main chain atoms (N) for ◆ 2H-nseries and ■ H-n_1 and H-n_3.

Fig. 7 shows a similar comparison, when an iso-free volume condition is applied. Also in this case a master curve can satisfactorily describe the whole series behaviour. Minor variations among different products could be attributed to structural diversification (i.e., number of repeating internal units).

The activation of viscous flow energy for 2H-nseries, H-n_1 and H-n_2 (Fig. 8) linearly increases with the number of carbon atoms in the chain (N), independently from the minor structural diversification between the two classes of compared products.

Fig. 9 shows the relationship between dielectric constant (ε) at 20 °C (1 kHz) and hydrogen content. The dielectric constant linearly depends on the total hydrogen content of the molecules, regardless the specific structure of the chain end. Thus, a common trend (i.e., a single master curve) describes the behaviour of H-n-series, 2H-n-series and HFPE-series, even if a certain scattering of data is observed, and the behaviour of the H-Z sample, lying on the same line, confirms the negligible effect of the number of functional groups per molecule on the dielectric constant.

The apparent deviation of the CH_3O-Z-series from this dependence should be confirmed by further experimental work.

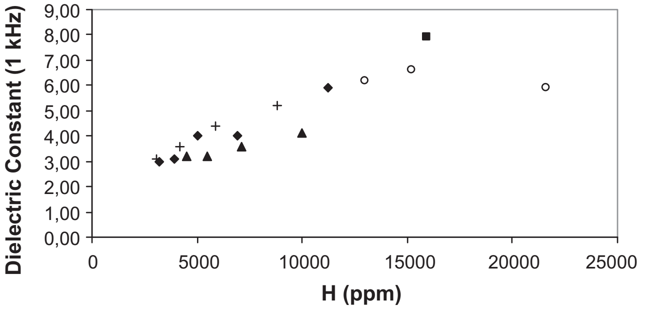

Fig. 9. Dependence of dielectric constant on H content at 1 kHz: ◆ H-n-series; ■ H-Z; ▲ 2H-n-series; × Y-series; * Z-series; + HFPE-series; ○ CH_3OZ-series.

3. Conclusions

The fundamental physical characterization of a new family of HFPEs, characterized by one $–OCF_2CH_3$ end group, has been carried out as a function of molecular weight. This evaluation has been extended to the analysis of contribution of other structural diversifications to the overall properties, with special reference to the presence of a second hydrogen containing end-groups ($–OCF_2CH_3$, or monohydroperfluoroalkyl) or monochloroperfluoroalkyl terminal group. The physical evaluation has been extended to similar perfluorinated or partially hydrogenated molecules for comparison. The results confirm the influence of molecular weight, perfluorinated structures and chain-ends on the specific property.

Accordingly to the literature, this characterization shows that, within each series, the contribution of end-groups vanishes at sufficiently high molecular weight, and becomes more and more important lowering the molecular weight. A comparison among the different series discussed in the present work clearly indicates that, in the region of high molecular weight, differences, if any, are due to the structural diversification of the internal perfluorinated chain (linear or branched). When lower molecular weights are compared some properties, namely cohesive energy density (CED) or molecular polarizability, can be strictly related to the presence of different end-groups. Viscosity data at room temperature are mainly ruled by the molecular weight, whereas structure plays a secondary role. However, the dependence of viscosity on the temperature is strongly related to the kind of end-groups present in the considered molecule, even if, when the comparison is made in iso-free volume condition, these differences largely disappear.

Among the different structures achievable thanks to this wide scope and original synthetic route, chlorine-free molecules can be selected. Thanks to the favourable reaction pathway and an easy modulation of physical properties, by varying the length and structure of the PFPE chain, these molecules could be considered as interesting candidates for a new generation of fluorinated fluids.

4. Experimental

4.1. Materials

The formulas of the samples studied in the present work, all from Solvay Solexis, have been given above. The structures of the products were determined by ^{19}F and ^{1}H NMR spectroscopy [38,39] and by GC/MS analysis; details of preparation and characterization of Series H-n and H-Z have been described in the discussion section or in a previous paper [24].

4.2. 2H-n series preparation

The samples belonging to the new 2H-n-series have been prepared starting from corresponding H-n-series. Depending on the molecular weight, i.e., boiling point, of the starting H-n-series precursors two different synthetic routes have been settled.

4.2.1. Materials for 2H-n-series

Galden® D100 [1/1 volume mixture of (*per*fluorobutyl)tetrahydrofurane and (*per*fluoropropyl)tetrahydropyrane, by Solvay Solexis] has been distilled immediately prior to use. 2-Propanol and sodium sulfate (from Aldrich Co.), Pd/C catalyst (10% Pd) (from Enghelard) and H_2 (from Mattheson) have been used as received.

4.2.2. Low boiling 2H-n_2 and 2H-n_3

The photo activated Cl abstraction has been performed in a photo-chemical unit which includes an immersion high-pressure Hanau mercury lamp (150 W), quartz jacketed and cooled by distilled water, and an outer Pyrex cylindrical reactor. This reactor

Table 3
NMR resonance signals of 2H-n_4 as determined by ^{19}F, ^{1}H and ^{13}C NMR.

Responding atoms	^{19}F NMR (δ ppm)	^{1}H NMR (δ ppm)	^{13}C NMR (δ ppm)
$\mathrm{CH_3}\mathit{CF_2}\mathrm{OCF(CF_3)CF_2\text{-}R}_f$	−62.0 (AB)[a]	–	123.4 (t, $J_{C\text{-}F}$ 272 Hz)
$\mathit{CF_3}\mathrm{CFHCF_2OCF(CF_3)CF_2\text{-}R}_f$	−75.8	–	118.3
$\mathrm{CF_3CFH}\mathit{CF_2}\mathrm{OCF(CF_3)CF_2\text{-}R}_f$	−78.9	–	116.9
$\mathrm{-CF(CF_3)CF_2OCF(}\mathit{CF_3}\mathrm{)CF_2H}$	−80.8	–	116.9
$\mathrm{-O}\mathit{CF_2}\mathrm{CF(}\mathit{CF_3}\mathrm{)O-}$	−79.2/−80.8	–	115.8/118.0
$\mathrm{-OCF(CF_3)}\mathit{CF_2}\mathrm{O\ CF_2CFHCF_3}$	−82.7	–	115.0
$\mathrm{-CF(CF_3)CF_2OCF(CF_3)}\mathit{CF_2H}$	−134.9	6.01	106.7 (td, $J_{C\text{-}F}$ 256 and 34 Hz)
$\mathrm{-CF(CF_3)CF_2O}\mathit{CF}\mathrm{(CF_3)CF_2H}$	−143.8	–	102.4
$\mathrm{-OCF_2}\mathit{CF}\mathrm{(CF_3)O-}$	−144.0 to −146.0	–	101.0 (dsix, $J_{C\text{-}F}$ 266 and 33 Hz)
$\mathrm{CF_3}\mathit{CFH}\mathrm{CF_2O-}$	−212	4.80	83.3 (dsix, $J_{C\text{-}F}$ 205 and 34 Hz)
$\mathit{CH_3}\mathrm{CF_2OCF(CF_3)CF_2\text{-}R}_f$	–	1.87	20.4 (t, $J_{C\text{-}F}$ 30 Hz)

[a] The broad signals make inaccurate the calculation of the coupling constant.

has been provided with magnetic stirring, cooling system (dry-ice/2-propanol), thermocouple, and inlet tube for withdrawing samples. In this photochemical unit (reactor of 0.5 l, optical path 1.5 cm) 108 g (0.25 mol) of H-n_2 and 156 g of 2-propanol have been charged.

The temperature during irradiation has been maintained at 20 °C in the reactor, and the conversion has been monitored by sampling as a function of time. After 7 h ^{19}F NMR analysis indicated a full conversion of the reagent to the expected product.

$\mathrm{Cl}\mathit{CF_2}\mathrm{CF(CF_3)O}$– $\mathrm{CF_3}\mathit{CF}\mathrm{(Cl)CF_2O}$– at −68.5 ppm and −140 ppm (vs. $CFCl_3$), respectively; and

$\mathrm{H}\mathit{CF_2}\mathrm{CF(CF_3)O}$– $\mathrm{CF_3}\mathit{CF}\mathrm{(H)CF_2O}$ at −135 ppm and −212 ppm (vs. $CFCl_3$), respectively.

The reaction mixture has been washed with diluted aqueous HCl (1% w/w) (2× 250 g), the bottom layer was separated, treated with sodium sulfate are fractionated on a 90 theoretical plates column.

91 g of 2H-n_2 (purity > 99%) were isolated (yield on isolated product 91%).

Similar procedure has been applied for the synthesis of 2H-n_3 product, which has been isolated with 90% yield.

4.2.3. High boiling 2H-n_4 and 2H-n_5

The higher boiling point of -n_4 and -n_5 products has allowed carrying out a catalytic hydrogenation of the labile C–Cl bond. In a three-necked 0.25 l flask, equipped magnetic stirrer, hydrogen inlet, gas outlet connected to a cooling condenser (at −80 °C), and thermometer, 140 g (0.183 mol) of H-n_4 and 3.0 g of Pd/C (Pd 10%) have been charged.

The temperature was raised at 190 °C by and external oil bath and the hydrogen has been fed at atmospheric pressure (ca. 10 l/h). After 4 h ^{19}F NMR analysis indicated a full conversion of the reagent to the expected product.

> $\mathrm{Cl}\mathit{CF_2}\mathrm{CF(CF_3)O}$– $\mathrm{CF_3}\mathit{CF}\mathrm{(Cl)CF_2O}$– at −68.5 ppm and −140 ppm (vs. $CFCl_3$), respectively; and
> $\mathrm{H}\mathit{CF_2}\mathrm{CF(CF_3)O}$– $\mathrm{CF_3}\mathit{CF}\mathrm{(H)CF_2O}$ at −135 ppm and −212 ppm (vs. $CFCl_3$), respectively.

The reaction mass has been cooled at room temperature and the catalyst filtered off.

By fractionation on a 90 theoretical plates column 120 g (0.164 mol, corresponding to a 90% yield) of 2H-n_4 have been isolated.

Similar procedure has been applied for the synthesis of 2H-n_5 product, which has been isolated with 88% yield.

4.3. Characterization

4.3.1. NMR

The following Table 3 summarizes all signals, acquired by ^{19}F, ^{1}H and ^{13}C NMR, related to product 2H-n_4. Interestingly, it must be noted that the two different mono-hydrogen substituted groups, –CF_2H and –CFH–, originate from the corresponding precursor that contains primary and secondary chlorine atoms.

4.3.2. GC/MS analysis

GC/MS analyses were performed on a HP 5890 gas chromatograph equipped with Porabond Q column (diameter 0.32 mm, length 25 m) coupled with a HP 5989 mass spectrometer.

4.3.3. Physicochemical characterization

Specific volumes at different temperatures have been measured by a conventional 2 ml dilatometer, with bulb and capillary section area purposely designed so as to secure accuracy higher than 0.0005 ml/g.

The glass transition temperatures have been measured using a differential scanning calorimeter Perkin-Elmer Pyris 1 (indium and cyclohexane calibrated). Samples have been cooled down to 110 K from room temperature at a rate of 80 K min^{-1}, and a scanning rate of 20 K min^{-1} has been chosen for the heating runs. The glass transition temperature (T_g) has been determined as the temperature corresponding to the midpoint of the heat capacity step measured in the heating run.

The kinematic viscosities have been measured following ASTM D 446 in a range between 253 K and 353 K. Two different Cannon Fenske capillary viscosimeters were used below 273 K, while a Cannon viscosimeter has been used for higher temperatures. The instruments have been calibrated at the testing temperatures with acetone, ethanol or the ASTM S3 oil.

The dielectric constant (ε) has been measured at 298 K and 1 kHz frequency with a Polymer Laboratories PL-DETA Analyzer equipped with a home made liquid cell in a parallel plate geometry with a guard ring. The dielectric constant has been determined as the ratio of the capacity of the cell filled with the sample and the capacity of the empty cell ($\varepsilon_{air} = 1$).

Acknowledgements

The authors wish to thank colleagues from Analytical and Material Science Dept., R&D Centre of Bollate for the characterization work, and Solvay Solexis for the permission to publish the present work.

References

[1] B.H. Wang, J.L. Adcock, S.B. Mathur, W.A. Van Hook, J. Chem. Thermodyn. 23 (1991) 699–710.
[2] V. Petrov, J. Fluorine Chem. 112 (2001) 117–121.
[3] G. Marchionni, R. Silvani, G. Fontana, G. Malinverno, M. Visca, J. Fluorine Chem. 95 (1999) 41–50.
[4] J.L. Adcock, M.L. Cherry, Ind. Eng. Chem. Res. 26 (1987) 208–215.
[5] J.L. Adcock, S.A. Kunda, D.R. Taylor, M.J. Nappa, A.C. Sievert, Ind. Eng. Chem. Res. 28 (1989) 1547–1549.
[6] J.L. Adcock, R.A. Beh, R.J. Lagow, J. Org. Chem. 40 (1975) 3271–3275.

[7] R.D. Chambers, B. Grievson, J. Fluorine Chem. 29 (1985) 323–339.
[8] S. Modena, P. Calini, G. Gregorio, G. Moggi, J. Fluorine Chem. 40 (1988) 349–357.
[9] R.D. Chambers, A.K. Joel, A.J. Rees, J. Fluorine Chem. 101 (2000) 97–105.
[10] A.L. Henne, M.A. Smook, J. Am. Chem. Soc. 72 (1950) 4378–4380.
[11] R.D. Chambers, S.L. Jones, S.J. Mullins, A. Swales, P. Telford, M.L.H. West, in: J.T. Welch (Ed.), ACS Symposium Series, vol. 456, 1991, p. 68, Washington, DC.
[12] M.G. Costello, US Patent 5741950 (1998).
[13] R.M. Flynn, M.W. Grenfell, G.G. Moore. J.G. Owens, D.S. Milbrath, WO 9622356 (1996).
[14] E.T. McBee, W.F. Marzluff, O.R. Pierce, J. Am. Chem. Soc. 74 (1952) 444–446.
[15] D.R. Vitcak, M.R. Flynn, US Patent 5750797 (1998).
[16] F.E. Behr, Y. Cheburkov, US Patent 6023002 (2000).
[17] M. Avataneo, U. De Patto, M. Galimberti, G. Marchionni, J. Fluorine Chem. 126 (2005) 633–640.
[18] W. Navarrini, M. Galimberti, G. Fontana, US Patent 7141704 (2006).
[19] M. Galimberti, G. Fontana, G. Resnati, W. Navarrini, J. Fluorine Chem. 126 (2005) 1578–1586.
[20] A.R. Ravishankara, S. Solomon, A.A. Turnipseed, R.F. Warren, Science 259 (1993) 194–199.
[21] R.A. Morris, T.M. Miller, A.A. Viaggiano, J.F. Paulson, S. Solomon, G.J. Reid, J. Geophys. Res. 100 (1995) 1287–1294.
[22] D. Sianesi, A. Marraccini, G. Marchionni, US Patent 5149842 (1992).
[23] G. Marchionni, P.A. Guarda, M. Paganin, US Patent 5488181 (1996).
[24] G. Marchionni, G. Spataro, E. Strepparola, Eur. Patent Appl. EP 695775 (1996).
[25] M. Visca, R. Silvani, G. Marchionni, Chem. Tech. 27 (2) (1997) 33–37.
[26] C. Tonelli, A. Meo.Di, R. Picozzi, J. Fluorine Chem. 128 (2007) 46–51.
[27] G. Marchionni, G. Ajroldi, G. Pezzin, in: S.L. Aggarwal, S. Russo (Eds.), Comprehensive Polymer Science, Second Supplement, Pergamon, London, 1996, pp. 347–388.
[28] G. Marchionni, M. Avataneo, U. De Patto, P. Maccone, G. Pezzin, J. Fluorine Chem. 126 (2005) 465–474.
[29] J.T. Hill, J. Macromol. Sci. Chem. A8 (3) (1974) 499–520.
[30] Y. Ohsaka, Petrotech (Tokyo) 8 (1985) 840–843.
[31] T.G. Fox, P.J. Flory, J. Appl. Phys. 21 (1950) 581–591.
[32] G. Marchionni, G. Ajroldi, M.C. Righetti, G. Pezzin, Macromolecules 26 (1993) 1751–1757.
[33] G. Marchionni, G. Ajroldi, M.C. Righetti, G. Pezzin, Polym. Commun. 32 (1991) 71–73.
[34] G. Marchionni, G. Ajroldi, P. Cinquina, E. Tampelli, G. Pezzin, Polym. Eng. Sci. 30 (1990) 829–834.
[35] G. Marchionni, M. Bassi, G. Fontana, P. Maccone, G. Ajroldi, J. Fluorine Chem. 98 (1999) 41–54.
[36] J.D. Ferry, Viscoelastic Properties of Polymers, third ed., Wiley, New York, 1980.
[37] G.C. Berry, T. Fox, Adv. Polym. Sci. 5 (1968) 261–357.
[38] M. Pianca, N. Del Fanti, E. Barchiesi, G. Marchionni, Chem. Today 13 (1995) 29–46.
[39] T.E. Karis, B. Marchon, D.A. Hopper, R.L. Siemens, J. Fluorine Chem. 118 (2002) 81–94.